Accepted Manuscript

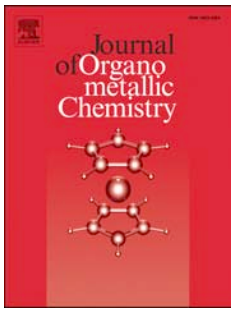

Photophysical and Biological Characterization of new cationic cyclometalated M(III) complexes of rhodium and iridium

Marion Graf , Yvonne Gothe , Nils Metzler-Nolte , Rafał Czerwieniec , Karlheinz Sünkel

PII: S0022-328X(14)00213-7

DOI: 10.1016/j.jorganchem.2014.04.031

Reference: JOM 18566

To appear in: *Journal of Organometallic Chemistry*

Received Date: 10 December 2013

Revised Date: 28 April 2014

Accepted Date: 29 April 2014

Please cite this article as: M. Graf, Y. Gothe, N. Metzler-Nolte, R. Czerwieniec, K. Sünkel, Photophysical and Biological Characterization of new cationic cyclometalated M(III) complexes of rhodium and iridium, *Journal of Organometallic Chemistry* (2014), doi: 10.1016/j.jorganchem.2014.04.031.

$[Ir(ptpy)_2(ddmp)]^+$

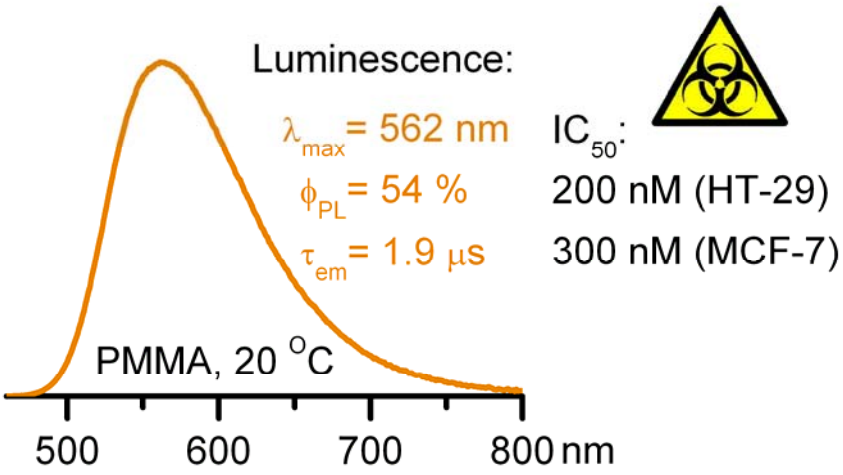

IC_{50}:

200 nM (HT-29)

300 nM (MCF-7)

$[Ir(ptpy)_2(ddmp)]^+$

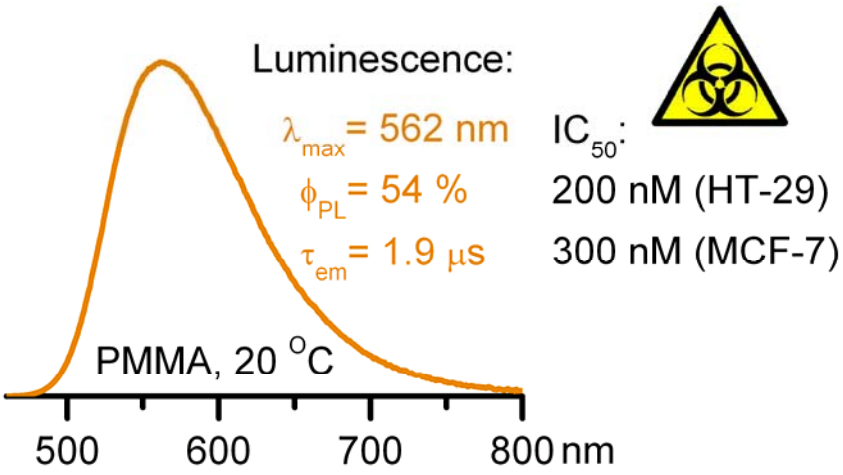

IC_{50}:

200 nM (HT-29)

300 nM (MCF-7)

Photophysical and Biological Characterization of new cationic cyclometalated M(III) complexes of rhodium and iridium

Marion Graf[a], Yvonne Gothe[b], Nils Metzler-Nolte[b], Rafał Czerwieniec[c] Karlheinz Sünkel[a*]

[a] *Department of Chemistry, Ludwig Maximilian University of Munich, Butenandtstraße 5–13, 81377 Munich, Germany*

[b]*Ruhr University Bochum, Universitätsstraße 150, 44801 Bochum, Germany*

[c]*Institute of Physical and Theoretical Chemistry Universität Regensburg, Universitätsstraße 31, 93053 Regensburg, Germany*

ABSTRACT

Synthesis and characterization of new cyclometalated complex salts $[M(ptpy)_2(ddmp)]PF_6$ (M = Rh, **1**; M = Ir, **2**; ptpy = 2-(*p*-tolyl)pyridinato; ddmp = 4,7-dichloro-2,9-dimethyl-1,10-phenanthroline) is described. Compounds **1** and **2** were obtained by the reaction of ddmp with the complexes $[\{M(\mu\text{-}Cl)(ptpy)_2\}_2]$ (M = Rh, Ir) in a mixture of CH_2Cl_2/MeOH/H_2O under reflux conditions. The compounds **1** and **2** crystallized from dichloromethane/chloroform/hexane in the triclinic space group $P\bar{1}$ and their molecular structures were confirmed by single-crystal X-ray diffraction. Compound **2** exhibits strong yellow phosphorescence in a polymer matrix and in solution at ambient temperature. Both compounds display significant cytotoxicity against human cancer cell lines with the IC_{50} values in the high nanomolar range.

---

* Corresponding author. Tel.: +49 89218077773; fax: +49 89218077774

E-mail address: suenk@cup.uni-muenchen.de (K. Sünkel)

Dedicated to Prof. Ingo –Peter Lorenz on the occasion of his 70th birthday

1. Introduction

Bis-cyclometalated Ir(III) complexes play an important role in the development of modern optoelectronic technologies (e.g. organic light emitting diodes – OLEDs [1] and light-emitting electrochemical cells – LEECs [2]), (bio-)–chemical labels and sensors [3]. In the last years we described the synthesis and characterisation of several neutral cyclometalated M(III) complexes of the elements rhodium and iridium [4], including complexes containing biomolecules as ancillary ligands [5].

It was found by several groups that for bio-medical diagnostic and therapeutic studies [3c, 6-9] the use of water-soluble complexes of the type $[M(C\hat{}N)_2(N\hat{}N)]^+$ was particularly beneficial. Starting from the long-known compounds with M = Rh [10] and Ir [11], C^N = 2-phenylpyridinato (ppy) and N^N = 2,2'-bipyridine (bpy) or phenanthroline (phen), numerous studies were performed to elucidate the effects of various substituents on the photophysical and electrochemical properties of the complexes and how they influence the device performance in different applications. [12-14]

In this paper we describe the synthesis and characterization of two new cyclometalated complex salts $[M(ptpy)_2(ddmp)]PF_6$ (M = Rh, **1**; M = Ir, **2**; ptpyH = 2-(*p*-tolyl)pyridine; ddmp = 4,7-dichloro-2,9-dimethyl-1,10-phenanthroline). The photophysical studies on the room-temperature luminescence of **2** as well as investigations of the cytotoxicity of **1** and **2** towards the cell lines MCF-7 and HT-29 are presented.

2. Experimental

2.1. General considerations

All manipulations were performed under an atmosphere of dry nitrogen using conventional Schlenk techniques. Solvents and Hptpy were used as received (from Aldrich). $[\{M(\mu\text{-}Cl)(ptpy)_2\}_2]$ (M = Rh, Ir) were prepared by our published method [4e, 4b]. NMR spectra were recorded in CD_2Cl_2 using a Jeol Eclipse 400 instrument operating at 400 MHz (^1H) and 100 MHz (^{13}C) respectively. Chemical shifts are given in ppm, referenced to the solvent signals at δ = 5.30 (^1H) or 53.8 ppm (^{13}C). Assignments of NMR signals refer to scheme 1. Mass spectra were measured using a Jeol Mstation JMS 700 spectrometer. Elemental analyses (C, H, N) were performed by the Microanalytical Laboratory of the Department of Chemistry, LMU Munich, using a Heraeus Elementar Vario El instrument.

Dulbecco's Modified Eagle's Medium (DMEM), containing 10% fetal calf serum, 1% penicillin and streptomycin, was used as growth medium. MCF-7 and HT-29 cells were detached from the wells with trypsin and EDTA, harvested by centrifugation and resuspended

again in the cell culture medium. The assays were carried out on 96 well plates with 6000 (3000) cells per well for MCF-7 (HT-29, respectively). After 24 h of incubation at 37°C and 10% CO_2, the cells were treated with the compounds **1** and **2** (with DMSO concentrations of 0.5%) with a final volume of 200 µl per well. For a negative control, one series of cells was left untreated. The cells were incubated for 48 h followed by adding 50 µl MTT (2.5 mg/ml). After an incubation time of 2 h, the medium was removed and 200 µl DMSO were added. The formazan crystals were dissolved and the absorption was measured at 550 nm, using a reference wavelength of 620 nm. Each test was repeated in quadruplicates in two independent experiments for each cell line.

((scheme 1))

*2.2. Synthesis of [Rh(ptpy)$_2$(ddmp)]PF$_6$ (**1**)*

To a solution of [{Rh(µ-Cl)(ptpy)$_2$}$_2$] (142 mg, 0.15 mmol) in 25 mL of a mixture of CH_2Cl_2/MeOH/H_2O (2:2:1) the ligand 4,7-dichloro-2,9-dimethyl-1,10-phenanthroline (110 mg, 0.4 mmol) was added and the mixture refluxed with stirring for 2 h. After cooling to room temperature KPF_6 (70 mg, 0.4 mmol) was added. The solvent was removed to dryness in vacuo and the residue dissolved in dichloromethane and chromatographed on alumina with CH_2Cl_2/acetone (9:1) as the eluent. The solution was evaporated to dryness and the residue was redissolved in 5 ml of dichloromethane and the product was precipitated by slow diffusion of hexane. X-ray quality crystals were obtained by slow diffusion of hexane into a solution of dichloromethane/chloroform of the compound at room temperature. Yield: 130 mg (50.4 %). *Anal.* Calc. for $C_{38}H_{30}Cl_2F_6N_4PRh$: C, 52.98; H, 3.51; N, 6.50. Found: C, 52.94; H, 3.78; N, 6.63 %. MS (FAB$^+$): *m*/*z* = 715.3 [M$^+$] complex cation. ^{1}H NMR: δ= 8.47 (s, 2 H, H_b), 7.96-7.78 (m, 4 H, H3 and H4), 7.71 (s, 2 H, H_f), 7.59 (d, 8 Hz, 2H, H8), 7.41 (“d”, 2H, H6), 6.92-6.86 (m, 4H, H5 and H9), 5.98 (s, 2H, H11), 2.15 (s, 6H), 2.05 (s, 6 H). ^{13}C {^{1}H} NMR: δ= 166.3 (d, 34 Hz, C12), 165.3 (C2), 165.1 (C_e), 149.3 (C6), 147.2 (C_a), 146.0 (C_d), 141.0, 140.9 (C7 and C10), 138.8 (C4), 133.9 (C11), 128.4 (C_f), 127.9 (C_c), 125.0, 124.9, 124.0 (C8, C9 and C_b), 122.9(C5), 120.2 (C3), 27.0 (C_g), 22.0 (C13).

*2.3. Synthesis of [Ir(ptpy)$_2$(ddmp)]PF$_6$ (**2**)*

To a solution of [{Ir(µ-Cl)(ptpy)$_2$}$_2$] (169 mg, 0.15 mmol) in 25 mL of a mixture of CH_2Cl_2/MeOH/H_2O (2:2:1) the ligand 4,7-dichloro-2,9-dimethyl-1,10-phenanthroline (110 mg, 0.4 mmol) was added and the mixture refluxed with stirring for 2 h. After cooling to

room temperature KPF_6 (70 mg, 0.38 mmol) was added. The solvent was removed in vacuo and the residue was dissolved in dichloromethane and chromatographed on alumina with CH_2Cl_2/acetone (9:1) as the eluent. The solution was evaporated to dryness and the residue redissolved in 5 ml of dichloromethane. The product was precipitated by slow diffusion of hexane. Suitable crystals for X-ray diffraction were obtained by slow diffusion of hexane into a solution of dichloromethane/chloroform at room temperature. Yield: 200 mg (66 %). *Anal.* Calc. for $C_{38}H_{30}Cl_2F_6IrN_4P$ x 0.5 $CHCl_3$: C, 45.76; H, 3.04; N, 5.54. Found: C, 46.00; H, 3.13; N, 5.66 %. MS (FAB^+): *m*/*z* = 805.4 [M^+] complex cation. NMR: δ= 8.49 (s, 2 H, H_b), 7.90 ("d", 8 Hz, 2 H, H3), 7.76 ("dt", 2 H, H4), 7.73 (s, 2 H, H_f), 7.57 ("d", 8 Hz, 2H, H8), 7.43 ("d", 2H, H6), 6.87 ("dt", 2H, H5), 6.83 ("dd", 2H, H9), 5.92 (s, 2H, H11), 2.12 (s, 6H, H_g), 2.07 (s, 6 H, H13). ^{13}C {^1H} NMR: δ= 167.9 (C2), 166.0 (C_e), 149.5 (C6), 149.1 (C_a), 148.2 (C12), 145.9 (C_d), 140.9 (C10), 140.8 (C7), 138.6 (C4), 132.5 (C11), 128.74 (C_f), 128.69 (C_c), 125.2 (C8), 124.4 (C_b), 124.0 (C9), 122.8 (C5), 119.9 (C3), 27.7 (C_g), 21.9 (C13).

2.4. X-ray structural determinations

Suitable single crystals of **1** and **2**, respectively, were selected by means of a polarization microscope, mounted on the tip of a glass fiber, and investigated on a BRUKER D8 Quest diffractometer using Mo Kα radiation (λ = 0.71073 Å). The intensities were corrected for absorption by the semi-empirical multiscan method (SADABS) [15]. The structure was solved by direct methods (SIR 97) and refined by full-matrix least-squares calculations on F^2 (SHELXL-97), as implemented in the software package WINGX.[16] Analysis by the program PLATON (also implemented in WINGX) showed large voids (33%) in the crystal of the Rh complex **1**, which was handled by implementing the program subroutine SQUEEZE. Anisotropic displacement parameters were refined for all non-hydrogen atoms. Details of the crystal data, data collection, structure solution, and refinement parameters are summarized in Table 1.

((*Table* 1))

2.5. Photophysical Measurements.

UV-Vis absorption spectra were recorded with a Varian Cary 300 double beam spectrometer. Luminescence and excitation spectra were measured with a Horiba Jobin Yvon Fluorolog 3 steady-state fluorescence spectrometer. For decay time measurements a PicoQuant LDH-P-C-375 pulsed diode laser (λ_{exc} = 372 nm, pulse width 100 ps) was applied as the excitation source. The emission signal was detected with a cooled photomultiplier attached to a FAST ComTec multichannel scalar card with a time resolution of 250 ps. Photoluminescence quantum yields were determined with a Hamamatsu C9920-02 system equipped with a Spectralon® integrating sphere. Diluted solutions ($c \approx 10^{-5}$ M^{-1}) in 2-methyltetrahydrofuran (MTHF) were degassed by several freeze-pump-thaw cycles (p = 1×10^{-5} mbar). Polymer films containing about 0.1 weight% of the Ir complex **2** were obtained by dissolving the emitter and poly(methyl methacrylate) (PMMA) in dichloromethane and spin-coating these solutions onto quartz glass substrates. PMMA films were measured under continuous flushing with nitrogen.

2.6. Computational Methodology.

Molecular geometry of $[It(ptpy)_2(ddmp)]^+$ (**2**) was optimized using the density functional theory (DFT) with the hybrid gradient corrected correlation functional B3LYP [17]. Electronic excitations were calculated for the DFT optimized ground-state geometry using the time-dependent density functional theory (TD-DFT). Six lowest triplet and singlet excitations

were computed. The Ahlrichs split-valence basis set SVP [18] was applied for atoms C, H, N, and Cl and the quadruple-dzeta quality basis set QZVP [19] was used for Ir. Inner-core electrons of Ir were substituted with a relativistic effective core potential. [20] All computations were carried out using the Gaussian 09 program package. [21]

3. Results and discussion

3.1. Synthesis and characterization of compounds

The cyclometalating ligand 2-(p-tolyl)pyridine (Hptpy) was used for the synthesis of the chloro-bridged dimers $[\{M(\mu\text{-}Cl)(ptpy)_2\}_2]$ (M = Rh, Ir) starting from the corresponding M(I) complexes $[\{M(\mu\text{-}Cl)(coe)_2\}_2]$ (coe = 1,4-cyclooctadiene) by an oxidative addition reaction as described previously [2b, 2e]. Subsequently, the preparation of the title complexes was realized by cleavage of the dimeric compounds to the cationic mononuclear complexes using the chelating ligand 4,7-dichloro-2,9-dimethyl-1,10-phenanthroline (ddmp). The reaction was carried out in a refluxing mixture of dichloromethane/methanol/water for 2 h. Thus, the complex salts $[M(ptpy)_2(ddmp)]Cl$ were formed. The salt metatheses with KPF_6 yielded the hexafluorophosphate derivatives **1** and **2** (see *Scheme*). The complex salts **1** and **2** were obtained as yellow crystals in good yields and were characterized by elemental analyses, ^1H and ^{13}C NMR spectroscopy, and by single crystal X-ray diffraction studies.

Due to strong overlap of the signals of the phenanthroline and the phenylpyridine moieties, both in the ^1H- and ^{13}C-NMR spectra, precise assignment of all the NMR signals to individual protons and carbon atoms in the aromatic region was not possible. The relative intensities of the methyl protons of the ptpy-and dmpp ligands being 6:6 prove the proposed stoichiometry.

((*scheme*))

*3.2. Crystal and molecular structure of **1** and* **2**

Crystals suitable for an X-ray diffraction study were grown from $CH_2Cl_2/CHCl_3$/hexane solutions. Crystals of **1** and **2**, respectively, belong to the triclinic space group $P\,\bar{1}$. The Rh compound **1** contains two independent molecules in the unit cell. As mentioned above, the analysis by the program PLATON showed large voids in the crystal of **1** which make up 33% of the unit cell volume. Since no solvent molecules could be localized, the program routine SQUEEZE was applied for simulating the missing electron density. This led to acceptable R1 values of ca. 6%, but left a high wR2 value of ca. 19%. The major difference

between the two independent molecules is found in the relative orientations of the three chelate rings: while the interplanar angles between the phenanthroline chelate and the two cyclometallates are 85±1° at Rh1, they are 80.6±0.8° at Rh2. The Rh-N(tpy) bond lengths are identical within 2σ, averaging at 2.042(4) Å. The same applies for the Rh-C(tpy) bonds (average 1.994(5) Å). The Rh-N(phen) bonds are longer at Rh1 (average 2.246(4) Å) than at Rh2 (average 2.225(5) Å), which reflects also the difference in the interplanar angles mentioned above. The N-M-C chelate angles range from 80.5(2)° to 81.6(2)°, while the N-M-N angle is identical on both Rh atoms within 1σ, averaging at 75.4(1)°. In the related bipyridine complex $[Rh(thpy)_2(bpy)]Cl$ bond lengths of 2.060 Å, 1.989 Å and 2.144 Å are found for Rh-N(thpy), Rh-C(thpy) and Rh-N(bpy), respectively[10c]. The chelate angle N-Rh-N is reported as 76.7(1)°.

((*figure* 1))

The Ir complex **2** (figure 1) crystallizes with two molecules of chloroform which could be localized without any problems. The Ir-N(tpy) bond lengths are identical within 2σ, averaging at 2.047(5) Å, which is only slightly longer than in the Rh compound. The Ir-C(tpy) and Ir-N(ddmp) bond lengths are identical within 1σ, averaging at 2.013(6) and 2.200(5) Å, respectively. Interestingly, the former bond is longer than in complex **1**, while the latter is shorter. The N-M-C chelate angles average at 80.6(2)° within 1σ, slightly smaller than in the Rh case, while the N-M-N chelate angle is with 75.9(2)° slightly larger than the Rh analog. The interplanar angles between the three chelate planes are identical within 2σ, averaging at 80.3(2)°. In both compounds the cyclometalated rings are close to ideally planar, while the phenanthroline chelate rings are better described as non-planar “envelopes”. In the related complex $[Ir(ppy)_2(dmdpbpy)][PF_6]$ (dmdpbpy = 6,6'-dimethyl-4,4'-diphenyl- bipyridine) bond lengths of ca. 2.04 Å, 2.01 Å and 2.21 Å are found for Ir-N(ppy), Ir-C(ppy) and Ir-N(dmdpbpy), respectively [2b] It was stated that the “ortho” methyl substituents, i.e. methyl groups in the positions 6 and 6’ of 2,2’-bipyridine and in the positions 2 and 9 of phenanthroline, lead to lengthening of the Ir-N(bpy) bonds as compared to the unsubstituted bpy complex. Also in the closely related complex $[Ir(ppy)_2(phen)][PF_6]$ the Ir-N(ppy), Ir-C(ppy) and Ir-N(phen) bond lengths of 2.05 Å, 2.01 Å and 2.14 Å were found, respectively. The latter Ir-N(phen) bonds are significantly shorter than the Ir-N(ddmp) distances of 2.200(5) Å in compound **2**. The bite angles at the cyclometallated ptpy and phenanthroline

moieties were reported as ca. 80° and 78°, respectively. [2a] Bulky substituents in more remote positions seemingly have no influence on the Ir-N(phen) bond lengths. [22]

*3.3. Photophysical properties of **1** and **2***

Luminescent transition metal (TM) complexes have become recognized as valuable luminophores for application in biological cell imaging studies. The accumulation of such bio-imaging agents in particular cell compartments can be monitored through confocal luminescence spectroscopy.[23-27] Phosphorescence stemming from the triplet excited state of a TM complex is distinctly red-shifted relative to the lowest absorption band which arises from a transition between the singlet ground state and the lowest singlet excited state. Thus, it can be easily distinguished from the autogenous cell fluorescence (mostly in the blue spectral region), which is characterized by relatively small Stokes' shifts, by wavelength filtering. Moreover, the relatively long decay times of the TM-complex phosphorescence (microseconds) differ from the short decay times (nanoseconds) of autogenous fluorescence by 2 to 4 orders of magnitude. Thus, the emission of a phosphorescent probe can be distinguished from the autofluorescence by the time-gated detection methods.[23] For these reasons we decided to investigate the photophysical properties of the Ir complex **2**.

The UV-Vis absorption spectra of **1** and **2** were studied in dichloromethane solution (c = 0.05 mM) at room temperature. The high-energy part of the spectra ($\lambda \leq 300$ nm) is dominated by spin-allowed $\pi \rightarrow \pi^*$ transitions of the ptpy and ddmp ligands. These overlapping ligand-centered transitions give rise to intense absorption bands peaking at λ_{max} = 272 nm ($\varepsilon_{max} = 1.8 \times 10^4$ $M^{-1}cm^{-1}$) for **1** and 274 nm ($\varepsilon_{max} = 5.0 \times 10^4$ $M^{-1}cm^{-1}$) for **2** (Fig. 1), respectively. In the lower energy region, between ca. 300 and 390 nm for complex **1** and between 300 and 430 nm for **2**, a series of weaker absorption bands ($\varepsilon \approx 3 - 8 \times 10^3$ $M^{-1}cm^{-1}$) with much weaker tails ($\varepsilon < 1000$ $M^{-1}cm^{-1}$) stretching at 390 – 450 nm (compound **1**) and 430 – 520 nm (compound **2**), respectively, is observed. The red tail of the absorption spectrum of **2** matches with the lowest-energy signals observed in the excitation spectrum recorded for this compound in a glassy solution at 77 K (Fig. 2). Since such absorptions are not present in the spectra of the free ligands ptpyH and ddmp, the long-wavelength absorption bands of the complexes are assigned to metal-to-ligand charge-transfer (MLCT) transitions involving the occupied d_π orbitals of the metals ($2d_\pi$(Rh) and $3d_\pi$(Ir) in **1** and **2**, respectively) and empty π^* orbitals of the ptpy and ddmp ligands, respectively. Similar arguments for the

assignment of the low-energy absorption bands of related TM-compounds can be found in numerous studies in the literature.[1c,28,29] The above assignments are further supported by results of the TD-DFT calculations described below.

((*figure* 2))

The Ir complex **2** is strongly luminescent at ambient temperature. For instance, $[Ir(ptpy)_2(ddmp)][PF_6]$ (**2**) doped into PMMA displays yellow luminescence with the maximum at λ_{max} = 562 nm. The emission band is broad and unstructured (Fig. 3). The quantum yield ϕ_{PL} amounts to 54 % and the decay time τ_{em} is 1.9 µs. Similar τ_{em} values in order of a few microseconds are frequently found for phosphorescent Ir(III) complexes. [1c, 28,29] Accordingly, the emission of **2** is assigned to the lowest triplet state T_1. Results of the TD-DFT computations point to the T_1 excited state being ^{3}MLCT in character with dominant contributions from the ddmp ligand. (See below.)

((*figure* 3))

The emission properties of **2** are modulated by the matrix/solvent used. Thus, solutions of $[Ir(ptpy)_2(ddmp)][PF_6]$ (**2**) in organic solvents show moderately intense orange emission. For instance, in 2-methyltetrahydrofuran (MTHF) the luminescence band is centered at λ_{max} = 612 nm. The quantum yield of this emission is 17 % and decay time τ_{em} = 0.56 µs (Table 3). According to the long excited-state lifetime and large diffusion rates in solution the photoluminescence of **2** is quenched by molecular oxygen. Thus, in air saturated solution the quantum yield decreases to 3.5 % and the decay time of τ_{em} = 140 ns is 4 times shorter than in the degassed solution. (Table 2) Nevertheless, the O_2-quenching is not complete and the luminescence of **2** remains reasonably strong for detection under aerobic conditions.

The observed red-shift of the emission band of **2** from λ_{max} = 526 nm in frozen MTHF at 77 K to 552 nm in PMMA at room temperature and λ_{max} = 612 nm in the MTHF solution is conform to the distinct charge-transfer character of the lowest excited state T_1 (^{3}MLCT). Thus, electrostatic interactions of the ^{3}MLCT-excited molecule with the induced dipole moments in its close surrounding result in an additional stabilization of the excited state and thus, to a lower energy of the emission. [30] The smaller separation between the emitting state T_1 and the ground state S_0 in solution, as compared to the PMMA matrix or the frozen MTHF glass at 77 K, leads to a stronger vibrational coupling between the T_1 and S_0 electronic states. As a result, according to the so-called energy gap law,[31] the non-radiative relaxation of the

T_1 excited state to the electronic ground state S_0 is more effective, which manifests itself by the distinctly lower ϕ_{PL} and τ_{em} values in solution.

((*Table* 2))

3.4. Theoretical calculations

The B3LYP/[SVP+QZVP(ECP)] DFT calculations were carried out on the $[Ir(ptpy)_2(ddmp)]^+$ ion (**2**) in order to elucidate the character of the lowest excited states and to ascertain the role of the particular ligands, ptpy and ddmp, respectively, for the excited-state properties of the complex. The HOMO and LUMO surfaces are illustrated in Fig. 4 and the characters of other spectroscopically relevant molecular orbitals are analysed in Table 3. The HOMO consists principally from a mixture of Ir-d_{x2-y2} and phenyl-π orbitals, whereas LUMO (π^*) is mainly localized on the ddmp ligand. Orbitals HOMO – 1 to HOMO – 3 contain dominant contributions from the phenyl fragments of the ptpy ligands and HOMO – 4 and HOMO – 5 represent essentially two 3d(Ir) orbitals. LUMO + 1 is mainly centred on ddmp and LUMO +2 and LUMO +3 are combined from dominant contributions from the pyridine rings of the both ptpy ligands.

((*Figure* 4))
((*Table* 3))

The lowest electronic transitions, $S_0 \rightarrow T_1$ and $S_0 \rightarrow S_1$, respectively, are identified as MLCT transitions, which originate mainly (98 %) in HOMO $\rightarrow$ LUMO excitations carrying distinct $3d_{x2-y2}$(Ir)-π^*(ddmp) character. The lowest singlet transition at 2.18 eV with the calculated oscillator strength *f* of only 0.0001 carries only very little intensity.[32] It contributes to the weak red tail of the absorption spectrum. On the other hand, the $S_0 \rightarrow S_2$ transition at 2.47 eV, which stems mainly from the HOMO $\rightarrow$ LUMO + 1 excitation (polarized along the C_2 axis of symmetry, which intersects the Ir atom and the centre of the ddmp ligand) is distinctly more intense (*f* = 0.0025) and, thus, it contributes strongly to the low-energy part of the absorption spectrum. A similar situation is frequently found in TM−diimine complexes, e.g. $Re(CO)_3(bpy)Cl$,[33] where the $S_0 \rightarrow S_1$ transition is very weak and cannot be spectrally resolved from the stronger $S_0 \rightarrow S_2$ MLCT transition.

3.5. Biological activity.

Ir(III) and Rh(III) complexes have recently gained considerable attention as anti-cancer agents.[3c, 6b] To obtain an insight into the anti-tumor activity of compounds **1** and **2**, their *in vitro* toxicity towards the cancer cell lines HT29 (human colon carcinoma) and MCF-7 (human breast carcinoma) has been investigated (Table 4). The cytotoxicity was evaluated using the MTT assay, which measures the mitochondrial metabolism in the entire cell. For the well-established clinical drug cisplatin, IC_{50} values (half maximal inhibitory concentration) of 7.0 ± 2.0 µM for HT-29 and 2.0 ± 0.3 µM for MCF-7, respectively, were obtained.[34]

((*Table* 4))

Compared to cisplatin, the investigated compounds show significantly higher cytotoxicity towards the cancer cell lines under study. These strong cytotoxic effects are reflected by relatively low IC_{50} values which are in the high nanomolar range. For a comparison, in a recent publication by Lo et al., IC_{50} of approximately 4 µM were reported for cyclometallated Ir compounds with dialkyl-amino substituted phenanthroline ligands [5c].

In general, the MCF-7 cells are more sensitive to the treatment than the HT-29 cells. Interestingly, the Ir(III) complex shows higher cytotoxicity towards both cell lines compared to its Rh(III) analogue. The opposite was reported in a previous work, [11] in which several Rh(III) and Ir(III) complexes were assayed for their cytotoxic activity. Containing the same ligand system, the Rh(III) complexes showed higher cytotoxicity than the Ir(III) analogues. This leads to the assumption that the cytotoxicity is not exclusively related to the metal center but also depends on the specific ligands present in a given complex type.

4. Conclusions

The synthesis of two cationic bis-cyclometalated complexes $[M(ptpy)_2(ddmp)][PF_6]$ (M = Rh, **1**; M = Ir, **2**; ptpy = 2-(p-tolyl)pyridinato, ddmp = 4,7-dichloro-2,9-dimethyl-1,10-phenanthroline) is described. These new metallorganic compounds were prepared in good yields by the bridge-splitting reaction between the dinuclear complexes $[\{M(\mu\text{-}Cl)(ptpy)_2\}_2]$ and the chelating diimine ligand ddmp. The X-ray diffraction studies revealed the cationic molecules of **1** and **2** as mononuclear M(III) complexes and, thus, confirmed the molecular structures of **1** and **2** inferred from the results of the elemental analyses and the spectroscopic NMR and MS investigations.

The iridium complex **2** is strongly luminescent as powder, polymer film, and in solution at ambient temperature. In PMMA it exhibits intense yellow emission centered at λ_{max} = 562 nm (ϕ_{PL} = 54%). In MTHF solution, this compound displays orange emission at λ_{max} = 612 nm, which is partly quenched by oxygen in non-degased samples. Nevertheless, even in aerated samples, the emission is reasonably strong (ϕ_{PL} = 3.5 % and τ_{em} = 140 ns) for a non complicated detection. The photophysical characterisations, supported by the results of the quantum mechanical computations, lead to the assignment of the observed luminescnce as stemming from the lowest triplet state T_1, which is mainly ^{3}MLCT (d(Ir)-π*(ddmp)) in character.

Both compounds under study are capable of penetrating living mammalian cells. In the human colon carcinoma HT-29 and the breast cancer MCF-7 cell lines strong cytotoxicity induced by **1** and **2** were observed. The half maximal inhibitory concentrations (IC_{50}) found for the both compounds are in the high nanomolar range (200 nM – 1000 nM). The cytotoxic effects of the iridium complex **2** slightly exceeded that of the rhodium congener **1**, i.e. the IC_{50} values for **2** were approximately three times smaller than that determined for **1**. Remarkably, the IC_{50} values of **2** are about one order of magnitude smaller than IC_{50} exhibited by the anticancer drug cisplatin under similar conditions against the same cell cultures.

Summing up, the rhodium and iridium complexes reported here are important for future biological/medicinal investigations making use of the luminescence and cytotoxic properties of these materials.

Acknowledgments

The authors are grateful to the Department of Chemistry of the Ludwig Maximilians University Munich for support. P. Mayer is acknowledged for collecting the X-ray crystal data data and Prof. Hartmut Yersin (University Regensburg) for inspiring discussions. R.C. thanks the German Federal Ministry of Education and Research (BMBF) for financial support.

Supplementary material

CCDC-975514 (**1**) and CCDC-975515 (**2**) contain the supplementary crystallographic data for this paper. These data can be obtained free of charge from The Cambridge Crystallographic Data Centre via http://www.ccdc.cam.ac.uk/data_request/cif.

Figure Captions:

Figure 1: Molecular structure of the cation of **2**. Thermal ellipsoids at the 30% probability level.

Figure 2. UV-Vis absorption spectrum of $[Ir(ptpy)_2(ddmp)][PF_6]$ (**2)** in CH_2Cl_2 (*c* = 0.05 mM) at room temperature (solid line) and 77 K excitation spectrum of 2 recorded in frozen MTHF (= 2-methyltetrahydrofuran) solution (dotted line), λ_{det} = 540 nm.

Figure 3. Luminescence spectra of $[Ir(ptpy)_2(ddmp)][PF_6]$ recorded in poly(methyl methacrylate) (PMMA, c = 1 weight%) and 2-methyltetrahydrofuran (MTHF, $c = 1 \times 10^{-5}$ M^{-1}) at ambient temperature. λ_{exc} = 400 nm.

Figure 4. Frontier orbitals of $[Ir(ptpy)_2(ddmp)]^+$ (**2**).

References

[1] (a) C.-H. Lin, Y.-C. Chiu, Y. Chi, Y.-T. Tao, L.-S. Liao, M.-R. Tseng, G.-H. Lee, Organometallics 31 (2012) 4349 and references therein;

(b) S.-K. Leung, K.Y. Kwok, K.Y. Zhang, K. K.-W. Lo, Inorg. Chem. 49 (2010) 4984 and references therein.

(c) H. Yersin, A. F. Rausch, R. Czerwieniec, T. Hofbeck, T. Fischer, Coord. Chem. Rev. 255 (2011) 2622 and references therein.

(d) K. K.-W. Lo, K. Y. Zhang, RSC Advances 2 (2012) 12069.

(e) B. Minaev, G. Baryshnikov, H. Agren, Phys. Chem. Chem. Phys. (2013) DOI: 10.1039/C3CP53806K and references therein.

[2] (a) R.D. Costa, E. Orti, H.J. Bolink, S. Graber, S. Schaffner, M. Neuburger, C.E. Housecroft, E.C. Constable, Adv. Funct. Mater. 19 (2009) 3456;

(b) R.D. Costa, E. Orti, D. Tordera, A. Pertegas, H.J. Bolink, S. Graber, C.E. Housecroft, L. Sachno, M. Neuburger, E.C. Constable, Adv. Energy Mater. 1 (2011) 282;

(c) R.D. Costa, E. Orti, H.J. Bolink, S. Graber, C.E. Housecroft, E.C. Constable, Chem. Commun. 47 (2011) 3207;

(d) R. D. Costa, E. Ortí, H. J. Bolink, F. Monti, G. Accorsi, N. Armaroli, Angew. Chem. Int. Ed. 51 (2012) 8178.

[3] (a) M. Schmittel, H. Lin, Inorg. Chem. 46 (2007) 9139

(b) H. Lin, M.E. Cinar, M. Schmittel, Dalton Trans., 39 (2010) 5130;

(c) P-K. Lee, W.H-T. Law, H-W. Liu, K. K-W. Lo, Inorg. Chem. 2011, 50, 8570;

(d) B.B.H. Leavens, C.O. Trindle, M. Sabat, Z. Altun, J.N. Demax, B.A. DeGraff, J. Fluoresc. 22 (2012) 163.

[4] (a) M. Graf, H.-C. Böttcher, K. Sünkel, Inorg. Chim. Acta 394 (2013) 363;

(b) H.-C. Böttcher, M. Graf, K. Sünkel, P. Mayer, H. Krüger, Inorg. Chim. Acta 365 (2011) 103;

(c) H.-C. Böttcher, M. Graf, K. Sünkel, H. Krüger, Inorg. Chim. Acta 370 (2011) 523;

(d) H.-C. Böttcher, M. Graf, K. Sünkel, B. Salert, H. Krüger, Inorg. Chem. Commun. 14 (2011) 377;

(e) K. Sünkel, M. Graf, H.-C. Böttcher, B. Salert, H. Krüger Inorg. Chem. Commun. 14 (2011) 539;

(f) M. W. Thesen, H. Krüger, S. Janietz, A. Wedel, M. Graf, J. Polym. Sci., Part A: Polym. Chem. 48 (2010) 389;

(g) M. Graf, M. Thesen, H. Krüger, P. Mayer, K. Sünkel, Inorg. Chem. Commun. 12 (2009) 701;

(h) M. W. Thesen, H. Krüger, S. Janietz, A. Wedel, M. Graf, J. Polym. Sci., Part A: Polym. Chem. 48 (2010) 389.

[5] (a) M. Graf, K. Sünkel, Inorg. Chim. Acta 371 (2011) 42;

(b) M. Graf, K. Sünkel, Inorg. Chim. Acta 379 (2011) 40;

(c) M. Graf, K. Sünkel, Inorg. Chim. Acta 387 (2012) 81.

[6] For recent reviews on bioactive iridium and rhodium complexes as therapeutic agents see:

(a) C-H. Leung, H-J. Zhong, D. S-H. Chan, D-L. Ma, Coord. Chem. Rev. 257 (2013) 1764, and references cited therein;

(b) Y. Geldmacher, M. Oleszak, W. S. Sheldrick, Inorg. Chim. Acta 393 (2012) 84-102

[7] C.-H. Leung, H.-J. Zhong, H. Yang, Z. Cheng, D. S.-H. Chan, V. P.-Y. Ma, R. Abagyan, C.-Y. Wong, D.-L. Ma, Angew. Chem. 124 (2012) 9144 ; Angew. Chem. Int. Ed. 51 (2012) 9010.

[8] P.-K. Lee, H.-W. Liu, S.-M. Yiu, M.-W. Louie, K. K.-W. Lo, Dalton Trans. 40 (2011) 2180.

[9] K. K.-W. Lo, C.-K. Li, K.-W. Lau, N. Zhu, Dalton Trans. (2003) 4682.

[10] (a) U. Mäder, T. Jenny, A. von Zelewsky, Helv. CXhim. Acta, 69 (1986) 1085;

(b) A. Zilian, U. Maeder, A. von Zelewski, H.U. Güdel, J. Amer. Chem. Soc. 111 (1989) 3855;

(c) U. Maeder, A. von Zelewsky, H. Stoeckli-Evans, Helv. Chim. Acta,75 (1992) 1320;

[11] A. P. Wilde, K.A. King, R.J. Watts, J. Phys. Chem. 95 (1991) 629

[12] K.P. Balashev, M.V. Puzyk, E.V. Ivanova, Russ. J. Gen. Chem. 81 (2011) 1547

[13] (a) C. Dragonetti, L. Falciola, P. Mussini, S. Righetto, D. Roberto, R. Ugo,, A. Valore, F. De Angelis, S. Fantacci, A. Scamellotti, M. Ramon, M. Muccini, Inorg. Chem. 46 (2007) 8553;

(b) E.C. Constable, C.E. Housecroft, P. Kopecki, C.J. Martin, I.A. Wright, J.A. Zampese, H.J. Bolink, A. Pertegas, Dalton Trans. 42 (2013) 8086

[14] (a) M.S. Lowry, W.R. Hudson, R.A. Pascal, Jr., S. Bernhard, J. Am. Chem. Soc. 126 (2004) 14129;

(b) J.I. Goldsmith, W.R. Hudson, M.S. Lowry, T.H. Anderson, S. Bernhard, J.Am.Chem.Soc. 127 (2005) 7502.

[15] SADABS V2008/1 (Bruker AXS Inc.)'

[16] (a) WINGX: Farrugia, L. J. J. Appl. Cryst. 32, (1999) 837.

(b) SIR 97: A. Altomare, M.C. Burla, M. Camalli, G.L. Cascarano, C. Giacovazzo, A. Guagliardi, A.G.G. Moliterni, G. Polidore, R. Spagna: J. Appl. Crystallogr. 32 (1999) 115.

(c) SHELX97: G.M. Sheldrick, Acta Crystallogr. A64 (2008) 112.

(d) PLATON: A. L. Spek, J. Appl. Cryst. 36 (2003). 7-13; Acta Cryst. D65 (2009) 148

(e) SQUEEZE - Sluis, P. v.d.; Spek, A. L. Acta Crystallogr., Sect A 46 (1990) 194

[17] (a) A. D. Becke, J. Chem. Phys., 98 (1993**)** 5648.

(b) P. J. Stephens, F. J. Devlin, C. F. Chabalowski, M. J. Frisch, J. Phys. Chem., 98 (1994**)** 11623.

[18] A. Schaefer, H. Horn, R. Ahlrichs, J. Chem. Phys., 97 (1992) 2571.

[19] F. Weigend, R. Ahlrichs, Phys. Chem. Chem. Phys., 7 (2005) 3297.

[20] (a) P. J. Hay, W. R. Wadt, J. Chem. Phys., 82 (1985) 270;

(b) P. J. Hay, W. R. Wadt, J. Chem. Phys., 82 (1985) 299.

[21] Gaussian09W, Version 8.0, M. J. Frisch, G. W. Trucks, H. B. Schlegel, G. E. Scuseria, M. A. Robb, J. R. Cheeseman, G. Scalmani, V. Barone, B. Mennucci, G. A. Petersson, H. Nakatsuji, M. Caricato, X. Li, H. P. Hratchian, A. F. Izmaylov, J. Bloino, G. Zheng, J. L. Sonnenberg, M. Hada, M. Ehara, K. Toyota, R. Fukuda, J. Hasegawa, M. Ishida, T. Nakajima, Y. Honda, O. Kitao, H. Nakai, T. Vreven, J. A. Montgomery, Jr., J. E. Peralta, F. Ogliaro, M. Bearpark, J. J. Heyd, E. Brothers, K. N. Kudin, V. N. Staroverov, R. Kobayashi, J. Normand, K. Raghavachari, A. Rendell, J. C. Burant, S. S. Iyengar, J. Tomasi, M. Cossi, N. Rega, J. M. Millam, M. Klene, J. E. Knox, J. B. Cross, V. Bakken, C. Adamo, J. Jaramillo, R. Gomperts, R. E. Stratmann, O. Yazyev, A. J. Austin, R. Cammi, C. Pomelli, J. W. Ochterski, R. L. Martin, K. Morokuma, V. G. Zakrzewski, G. A. Voth, P. Salvador, J. J. Dannenberg, S. Dapprich, A. D. Daniels, Ö. Farkas, J. B. Foresman, J. V. Ortiz, J. Cioslowski, and D. J. Fox, Gaussian, Inc., Wallingford CT, 2009.

[22] E.g. with a 9,9-dihexylfluorene substituent in „meta“ position a Ir-N(phen) bond of ca. 2.15 Å was found: C. Rothe, C-J. Chiang, V. Jankus, K. Abdullah, X. Zeng, R. Jitchati, A.S. Batsanov, M.R. Bryce, A.P. Monkman, Adv. Funct. Mater. 19 (2009) 2038.

[23] S. W. Botchway, M. Charnley, J. W. Haycock, A. W. Parker, D. L. Rochester, J. A. Weinstein, J. A. G. Williams, Proc. Nat. Acad. Sci. USA 105 (2008) 16071.

[24] R. G. Balasingham, F. L. Thorp-Greenwood, C. F. Williams, M. P. Coogan, S. J. A. Pope, Inorg. Chem. 51 (2012) 1419.

[25] Q. Zhao, C. Huang, F. Li, Chem. Soc. Rev. 40 (2011) 2508.

[26] P. Wu, E. L.-M. Wong, D.-L. Ma, G. S.-M. Tong, K.-M. Ng, C.-M. Che, Chem. Eur. J. 15 (2009) 3652.

[27] K. Kowalski, L. Szupak, R. Czerwieniec, Tytus Bernas, *manuscript in preparation*.

[28] T. Hofbeck, H. Yersin, Inorg. Chem. 49 (2010) 9290.

[29] M. Graf, R. Czerwieniec, K. Sünkel, Z. Anorg. Allg. Chem. 639 (2013) 1090.

[30] C. Reichardt, Solvents and Solvent Effects in Organic Chemistry, 3rd ed., WILEY-VCH, Weinheim, 2003,. pp. 352.

[31] J. V. Caspar, T. J. Meyer, J. Phys. Chem. 87 (1983) 952.

[32] The lowest-energy electronic transitions in $[Ir(ptpy)_2(ddmp)]^+$ (molecular symmetry group C_2) are associated with promotion of an electron from Ir onto the ddmp ligand along the C_2 symmetry axis (= x-axis of coordinates). Thus, they result in a significant change of the molecular dipole moment along this axis. In such a situation, the transition matrix element $\langle f_1 | e\vec{r}_x | f_2 \rangle$, where f_1 and f_3 are the molecular wavefunctions of the initial and the final quantum states, is intuitively expected to be significantly larger than the transition matrix elements $\langle f_1 | e\vec{r}_y | f_2 \rangle$ and $\langle f_1 | e\vec{r}_z | f_2 \rangle$ orthogonal to the C_2 axis. ($e\vec{r}_x$, $e\vec{r}_y$, $e\vec{r}_z$ are the molecular dipole moment components.) HOMO of $[Ir(ptpy)_2(ddmp)]^+$ carries distinct Ir-d_{x2-y2} character and belongs to the symmetry type *a*. LUMO is a *b* type ddmp-π* orbital and LUMO + 1 is an *a* type ddmp-π* orbital, respectively. In the C_2 point group, $\langle f_1 | e\vec{r}_x | f_2 \rangle$ elements involving f_1 and f_3 spanning different irreducible representations are equal zero. Therefore the HOMO → LUMO transition described by the matrix element $\langle a | e\vec{r}_x | b \rangle = 0$ is expected to carry only very little intensity. On the contrary, the HOMO → LUMO + 1 transition ($\langle a | e\vec{r}_x | a \rangle \neq 0$) is expected to be more intense. Indeed, the oscillator strengths calculated for the HOMO → LUMO and HOMO → LUMO + 1 excitations are $f = 0.0001$ and $f = 0.0025$, respectively.

[33] A. Caniizzo, A. M. Blanco-Rodríguez, A. E. Nahhas, J. Šebera, S. Záliš, A. Vlček Jr., M. Chergui, J. Am. Chem. Soc. 130 (2008) 8967.

[34] M. Harlos, I. Ott, R. Gust, H. Alborzinia, S. Wolfl, A. Kromm and W. S. Sheldrick, J. Med. Chem. 51 (2008) 3924

Table 1: Experimental Data of the Structure determinations

Compound	**1**	**2**
Empirical formula	$C_{38}H_{30}Cl_2F_6N_4PRh$	$C_{38}H_{30}Cl_2F_6IrN_4P \times 2CHCl_3$
Formula weight	861.44	1189.47
Temperature K	200(2)	200(2)
Crystal system	Triclinic	Triclinic
Space group	P -1	P -1
Unit cell dimensions		
a [Å]	13.714(7)	10.494(5)
b [Å]	17.332(9)	13.560(6)
c [Å]	22.395(12)	16.705(8)
α	106.308(16)°.	71.398(5)°.
β	99.64(3)°.	81.95(2)°.
γ	107.499(17)°.	γ = 77.448(18)°.
Volume [$Å^3$]	4684(4)	2195.0(15)
Z	2 * 2	2
Density (calculated) [Mg/m^3]	1.222	1.802
Absorption coefficient [mm^{-1}]	0.564	3.630
F(000)	1736	1164
Crystal size [mm^3]	0.215 × 0.102 × 0.062	0.186 × 0.053 × 0.04
Theta range for data collection	2.43 to 25.36°.	2.32 to 25.76°.
Index ranges	-16≤h≤16, -20≤k≤20, -26≤l≤26	-12≤h≤12, -16≤k≤16, -20≤l≤20
Reflections collected	85022	39640
Independent reflections [R_{int}]	17146 [0.0497]	8338 [0.0731]
Completeness	98.5 %	99.0 %
Absorption correction	Semi-empirical from equivalents	
Max. and min. transmission	0.6462 and 0.5878	0.4291 and 0.3523
Data / parameters	17146/ 945	8338 / 545
Goodness-of-fit on F^2	0.803	1.037
Final R indices [I>2sigma(I)]	R1 = 0.0571, wR2 = 0.1875	R1 = 0.0415, wR2 = 0.0855
R indices (all data)	R1 = 0.0771, wR2 = 0.2034	R1 = 0.0669, wR2 = 0.0950
Largest diff. peak and hole [$e.A^{-3}$]	2.232 and -0.887	1.204 and -1.282

Table 2. Luminescence properties of $[Ir(ptpy)_2(ddmp)][PF_6]$ (**2**).

Solvent [Temperature]	Emission maximum λ_{max}	Quantum yield ϕ_{PL}	Decay time τ_{em}
MTHF [300 K], O_2-free [a]	612 nm	17 %	560 nm
MTHF [300 K], air saturated	612 nm	3.5 %	140 ns
MTHF [77 K]	526 nm [b]		7.2 µs
PMMA [300 K] [c]	562 nm	54 %	1.9 µs

a) The sample was degassed under vacuum by several freeze-pump-thaw cycles; $p = 10^{-5}$ mbar.
b) The spectrum measured at 77 K is structured with a distinctly resolved shoulder at 560 nm.
c) Measured under N_2.

Table 3. Percent contributions from the Ir atom, ddmp, and ptpy ligands to the highest occupied orbitals (lying within 1 eV below the HOMO energy) and the lowest virtual orbitals (lying within 1 eV above the LUMO energy) of $[Ir(ptpy)_2(ddmp)]^+$ (**2**). The Mulliken population analysis was performed for the ground-state Kohn-Sham orbitals resulting from the B3LYP/[SVP+QZVP(ECP)] DFT calculations.

Orbital	Energy (eV)	Ir (%)	ptpy1 (%)	ptpy2 (%)	ddmp (%)
HOMO – 5	-8.956	66	14	15	6
HOMO – 4	-8.877	59	10	11	21
HOMO – 3	-8.816	1	43	44	11
HOMO – 2	-8.693	11	41	42	6
HOMO – 1	-8.373	1	47	47	5
HOMO	-7.894	29	34	34	3
LUMO	-5.164	3	1	11	85
LUMO + 1	-4.916	1	1	4	95
LUMO + 2	-4.272	5	46	46	3
LUMO + 3	-4.188	5	47	47	1

Table 4: Cytotoxicity data

Compound	Cell line	IC_{50}/μM
$[Rh(ptpy)_2(dmpp)](PF_6)$ (**1**)	HT-29	0.5 ± 0.1
	MCF-7	1.0 ± 0.3
$[Ir(ptpy)_2(dmpp)](PF_6)$ (**2**)	HT-29	0.2 ± 0.1
	MCF-7	0.3 ± 0.1

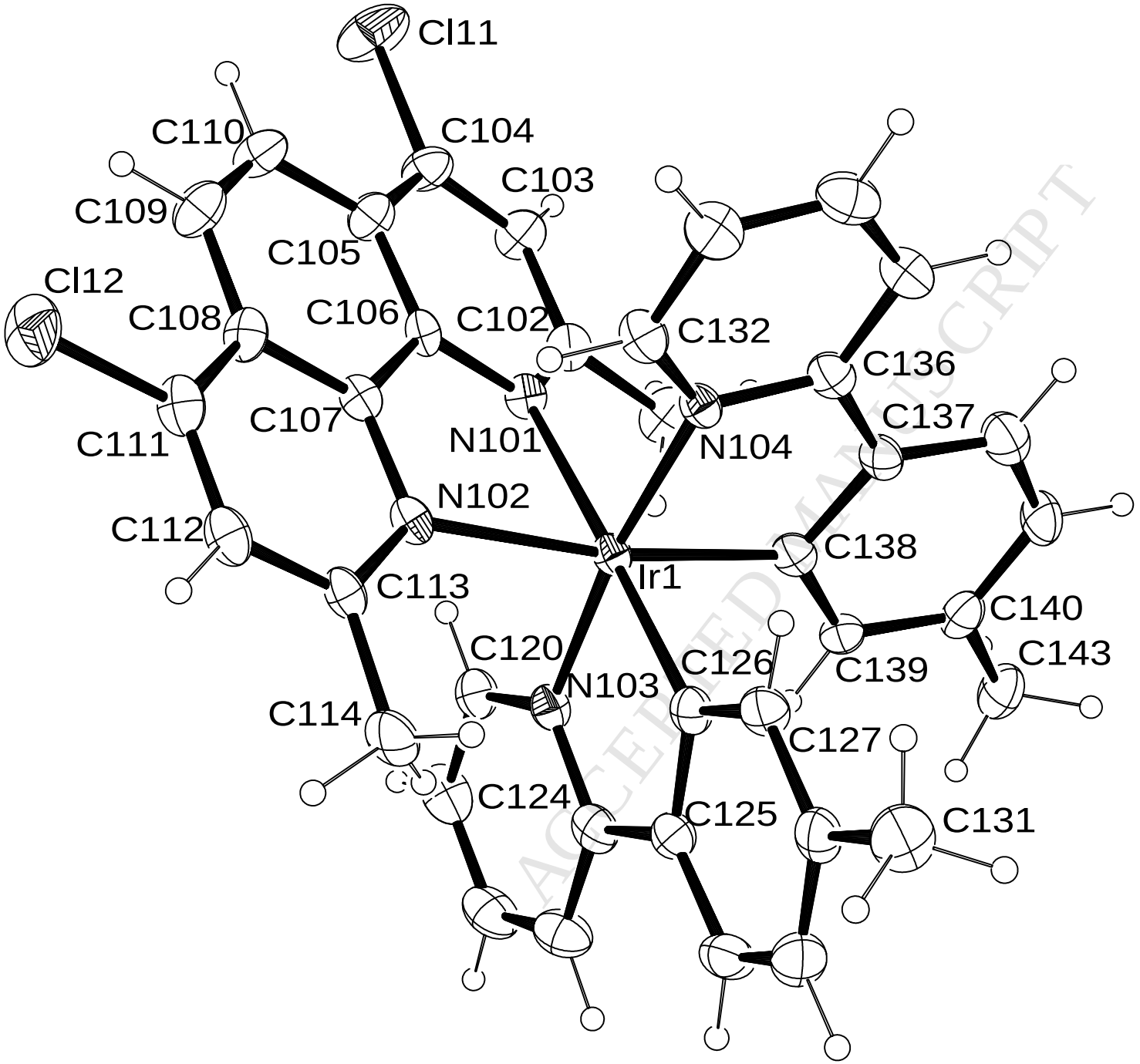

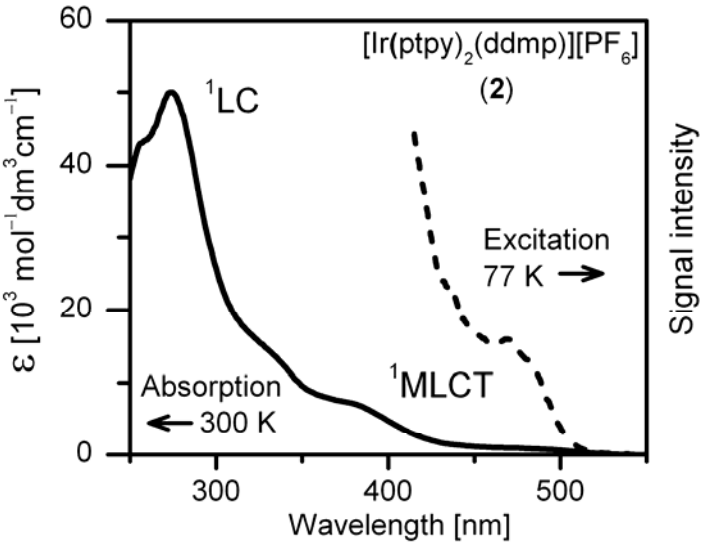

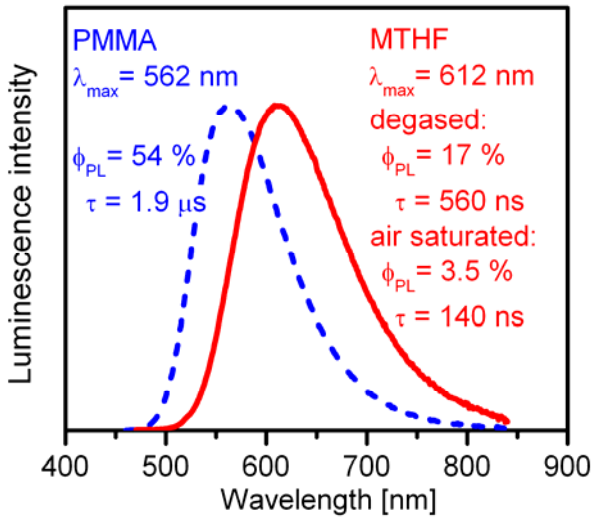

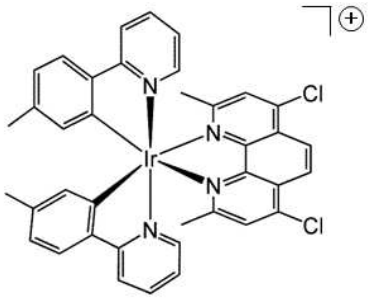

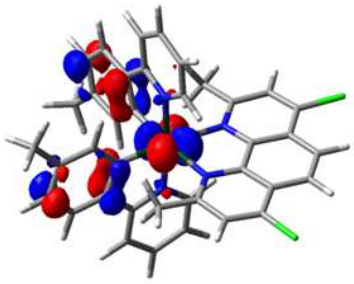

HOMO

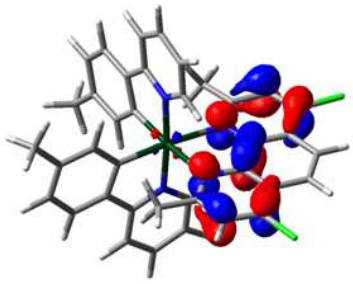

LUMO

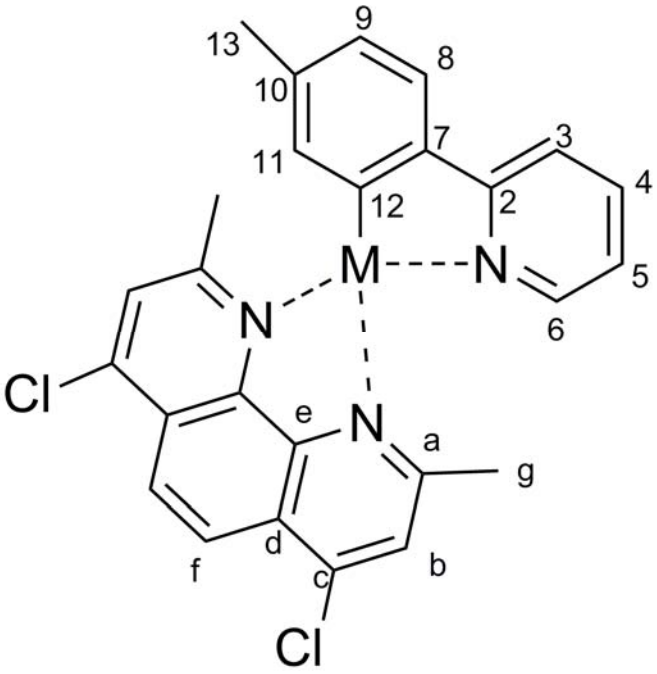

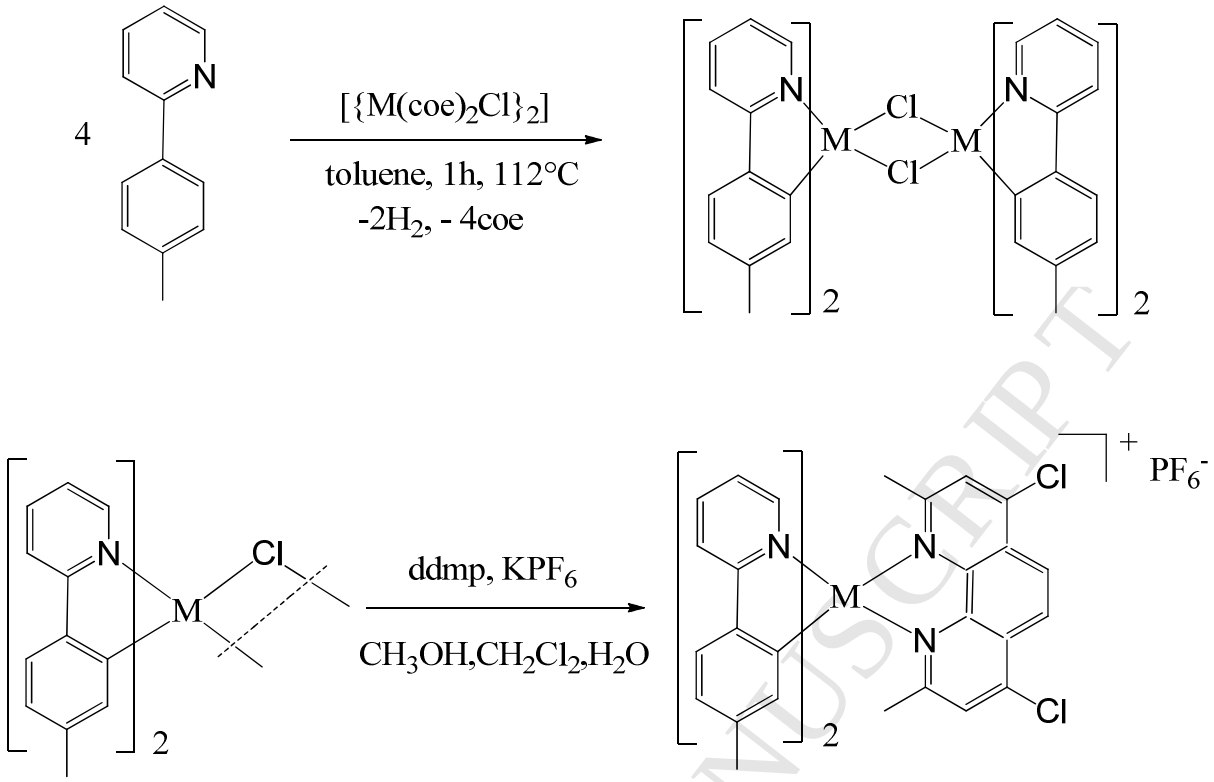

M = Rh, Ir; ddmp = 4,7-Dichloro-2,9-dimethyl-1,10-phenanthroline

HIGHLIGHTS

- new cyclometalated complexes $[M(ptpy)_2(ddmp)]PF_6$ (M = Rh, **1**; Ir, **2**) were prepared
- both molecular structures were confirmed by single-crystal X-ray diffraction.
- **2** phosphoresces yellow in a polymer matrix and in solution at ambient temperature.
- **1** and **2** show significant cytotoxicity against human cancer cell lines.